

NEA/NSC(93)9

**NEA-NSC 3-D /1-D PWR CORE TRANSIENT BENCHMARK  
UNCONTROLLED WITHDRAWAL OF CONTROL RODS AT  
ZERO  
POWER**

**Final Specifications**

by

**Roger FRAIKIN  
TRACTEBEL ENERGY ENGINEERING  
Brussels, Belgium**

and

**Herbert Finnemann  
SIEMENS AG/KWU  
Erlanger, Germany**

**September 1993**

**OECD Nuclear Energy Agency**

OECD/NEA  
**3-D LWR CORE TRANSIENT BENCHMARK (3DLWRCT)**  
Uncontrolled Withdrawal of Control Rods at Zero Power  
(NEA/NSC/DOC(93) 9 - May 1993)

**Intention to Participate**

To be returned by 15 June 1993 a copy each to

Roger FRAIKIN  
TRACTEBEL  
avenue Ariane 7  
B-1200 Bruxelles  
Belgium

and

Enrico SARTORI  
OECD/NEA  
12 bd des Iles  
F-92130 Issy les Moulineaux  
France

fax: +32 (2) 773 8900  
email: fraikin@tractebel.be

+33 (1) 4524 1110  
sartori@nea.oecd.circe.fr  
sartori@frnab51.bitnet

I intend to participate in this extension to the 3D LWR Core Transient benchmark concerning uncontrolled withdrawal of control rods at zero power in PWRs. I enclose my comments on the draft benchmark specification.

Name: .....

Address: .....

.....

.....

Computer code(s) that will be used: .....

Bibliographic reference: .....

.....

.....

For new participants only:

I wish to receive the data for the specification on:

Diskette: 3 1/2 " MSDOS  5 1/4 " MSDOS

via e-mail; address: .....

*( Please add comments on separate sheet)*

**NEA-NSC 3-D/1-D PWR CORE TRANSIENT BENCHMARK  
UNCONTROLLED WITHDRAWAL OF CONTROL RODS AT ZERO POWER**

**TABLE OF CONTENTS**

	Page
<b>1. INTRODUCTION</b>	<b>3</b>
<b>2. REFERENCE PRESSURIZED WATER REACTOR</b>	<b>4</b>
2.1 General	4
2.2 Core Geometry	4
2.3 Neutron modelling	4
2.4 Macroscopic Cross Sections and Derivatives	4
2.5 Composition Map	5
2.6 Doppler Temperature	5
2.7 Subassembly Geometry	5
2.8 Thermophysical Properties	6
2.9 Neutronics-Thermohydraulics Coupling	6
2.10 Operation Data	6
2.11 Heat Exchange Correlations	6
2.12 Pressure Drops	6
<b>3. PROBLEM DESCRIPTION</b>	<b>7</b>
3.1 Nature of the problem	7
3.2 Calculations of the Initial Steady State	7
3.3 Transient calculations	7
3.4 Rods configuration	7
<b>4. OUTPUT DESCRIPTION</b>	<b>8</b>
4.1 Initial steady state	8
4.2 Transient core averaged results (time histories)	8
4.3 Transient hot pellet results (time histories)	8
4.4 Snapshots at time of power maximum	9
<b>5. OUTPUT FORMAT</b>	<b>10</b>
5.1 General information	10
5.2 Output sample	10
<b>6. TABLES</b>	<b>13</b>
<b>7. FIGURES</b>	<b>20</b>

## 1. INTRODUCTION

This benchmark is an extension of the NEACRP PWR 3-D core transient benchmark (rod ejection accident) described in NEACRP-L-335 (Rev.1) document, and is based on the same core model. Actually, the "Uncontrolled Withdrawal of Control Rods at Zero Power" accident on a PWR requires very similar data to the rod ejection one, the main difference lying in the dynamic evolution.

This accident consists basically in a continuous reactivity insertion, limited by a reactor trip, which occurs a certain delay after high flux or high flux increase detection. Like the rod ejection accident, the peak power usually occurs before the scram and the main factor limiting the consequences of the accident is the Doppler effect. The temperature rise, however, is stopped by the trip, that must therefore be taken into account. It should be noted that the peak power occurs while important power distribution changes take place in the core, because the rod extraction continues until reactor trip.

1-D as well as 3-D methods are invited, and the output set includes global, axial and 3-D results. Local parameters refer to the finest available flux distribution, since most modern codes use fine-flux reconstruction methods.

Safety-related output are to be provided, such as hot pellet fuel enthalpy, maximum fuel temperature and maximum cladding temperature.

Time history of heat exchange coefficient between moderator and cladding in hot pellet will help to identify possible Thermal & Hydraulic correlations influence.

The authors would like to thank MM Hutt and Daudin for their valuable comments on the preliminary specifications.

## 2. REFERENCE PRESSURIZED WATER REACTOR

### 2.1 General

The reference scheme for Pressurized Water Reactors (PWRs) is derived from real reactor geometry and operation data.

The set of data given in the following paragraphs and in the pertinent tables and figures, completely defines the four benchmark exercises.

### 2.2 Core Geometry

The radial geometry of the reactor core is shown in Figure 2.1. Radially, the core is divided into cells 21.606 cm wide, each corresponding to one fuel assembly (FA), plus a radial reflector cell (shaded area) of the same width. Axially, the reactor core is divided into 16 layers with heights of 7.7, 11.0, 15.0, 30.0 (10 layers), 12.8 (2 layers), and 8.0 cm, (from bottom to top), adding up to a total height of the active core of 367.3 cm. Upper and lower axial reflector have thicknesses of 30.0 cm.

The mesh used for calculations is up to the participant, according to the numerical capabilities of the code. Output should however give volume averaged results on the specified mesh.

Fuel assemblies with different U-235 enrichments and different numbers of burnable absorbers rods are present in the core. The axial and radial distributions of the enrichment and absorbers can be found in chapter 2.4.

The radial arrangement of control assemblies (CA) is shown in Figure 2.2. The total CA length, which coincides with the absorber length, is 362.159 cm. The driver device section following the top of the absorber is distinguished from the absorber via a different cross section data set. No tip of control rods is defined. The position of the lower CA absorber edge from the bottom of the lower reflector is 37.7 cm for a completely inserted CA, and 401.183 cm for a completely withdrawn CA. Measured in units of steps, complete insertion and withdrawal of a CA correspond to 0 and 228 steps, respectively.

Participants to the former benchmark will note that the central control cluster added for symmetry in the rod ejection problem has been removed for this new benchmark.

### 2.3 Neutron Modelling

Two prompt neutron groups, i.e. thermal and fast neutrons, and six delayed neutron groups are used for neutron modelling. The boundary condition for the solution of the neutron diffusion equation is flux vanishing at the outer reflector surface.

Velocities and the energy release per fission for the two prompt neutron groups are given in Table 2.1, and are considered to be independent of time and space. Table 2.2 shows the time constants and fractions of delayed neutrons.

Delays are neglected in energy releases. The thermal energy output is to be released for 98.1 % in the fuel and for 1.9 % in the coolant.

### 2.4 Macroscopic Cross Sections and Derivatives

A complete set of macroscopic cross sections for transport, scattering, absorption and fission and their derivatives with respect to the boron density, moderator temperature, moderator density, and fuel temperature is defined for each composition. Table 2.4 shows the definition of all cross sections, derivatives, and reference values associated with a composition. In addition, all cross section data will be supplied on diskettes.

Let  $\rho$  be the water density,  $T_F$  the Doppler temperature (in K),  $c$  the boron concentration (in ppm), and  $T_M$  the moderator temperature (in °C). Any macroscopic cross-section  $\Sigma$  must be calculated according to the formula

$$\Sigma = \Sigma_0 + (\partial\Sigma/\partial\rho)_0 (\rho - \rho_0) + (\partial\Sigma/\partial\sqrt{T_F})_0 (\sqrt{T_F} - \sqrt{T_{F,0}}) + (\partial\Sigma/\partial c)_0 (c - c_0) + (\partial\Sigma/\partial T_M)_0 (T_M - T_{M0})$$

where subscript "o" denotes the reference values  $\rho_0$ ,  $T_{F,0}$ ,  $c_0$  and  $T_{M,0}$  and the reference point  $(\rho_0, T_{F,0}, c_0, T_{M0})$ .

The cross section at a numerical node with CA can be determined by simply adding a constant cross section increment  $\Delta\Sigma_{CA}$  contributed from the CA to the cross section without CA:

$$\Sigma_{\text{with CA}} = \Sigma_{\text{without CA}} + p \Delta\Sigma_{CA}$$

where  $p$  is the relative insertion in the node ( $0 \leq p \leq 1$ ). The use of a more accurate formula for partly inserted rods is recommended. The contribution of the CA driver is treated in an analogous way. The incremental cross section for the CAs and for their drivers are given in Table 2.5 with the same key as in Table 2.4.

Two types of absorbers are defined, according to the type of concerned fuel assembly:

- absorber "type 1": in 2.1% enriched FAs;
- absorber "type 2": in 3.1% FAs.

## 2.5 Composition Map

Within the core geometry, 11 different compositions and the corresponding sets of cross sections are defined. The definition of the compositions can be seen in Table 2.3. Each space cell of the reactor geometry can be related to one of these compositions. The axial and radial locations of the compositions within the reactor geometry are shown in Figures 2.3 through 2.5. The values of cross sections and derivatives which are associated with each composition are defined in Tables 2.6.1 through 2.6.11. The key to these tables is explained in Table 2.4.

## 2.6 Doppler Temperature

The Doppler temperature  $T_F$  is found from the fuel temperature at the fuel rod center  $T_{F,C}$  and the fuel rod surface  $T_{F,S}$  via the relation

$$T_F = (1 - \alpha) T_{F,C} + \alpha T_{F,S}$$

where  $\alpha$  is taken equal to 0.7.

## 2.7 Subassembly Geometry

The geometrical data for the FA are given in Table 2.7. For the neutronic problem, FA are considered as homogeneous.

## 2.8 Thermophysical Properties

The UO<sub>2</sub> density without dishing is 10.412 g/cm<sup>3</sup> (95 % of the theoretical density) at a temperature of 20°C. The pellet dishing amounts to 1.248 %. The cladding material is Zirkaloy-4 with a density of 6.6 g/cm<sup>3</sup>.

Participants of the benchmark should use the following reference relations for the heat conductivity  $\lambda$  (W/m<sup>2</sup>°K) and specific heat capacity  $C_p$  (J/kg.K) of fuel and cladding

$$\lambda_{\text{UO}_2} = 1.05 + 2150 / (T - 73.15)$$

$$\lambda_{\text{Zirkaloy-4}} = 7.51 + 2.09 \cdot 10^{-2} T - 1.45 \cdot 10^{-5} T^2 + 7.67 \cdot 10^{-9} T^3$$

$$C_{p,\text{UO}_2} = 162.3 + 0.3038 T - 2.391 \cdot 10^{-4} T^2 + 6.404 \cdot 10^{-8} T^3$$

$$C_{p,\text{Zirkaloy-4}} = 252.54 + 0.11474 T$$

where T is the temperature (°K).

Enthalpy of UO<sub>2</sub> is given by  $C_p$  UO<sub>2</sub> integration between 0°K and T.

Expansion effects of fuel and cladding will not be considered in this benchmark.

## 2.9 Neutronic-Thermohydraulic Coupling

The feedback or coupling between neutronics and thermohydraulics is characterized by definition of channel regions. In the present work, each FA has to be defined as a channel region ("closed channels" model), ignoring inter-assembly cross-flow and mixing, and using one T&H feedback axial mesh per assembly.

A flat profile of the radial distribution of the power density inside the fuel shall be assumed for the T&H problem.

The inlet mass flow through the core given in Table 2.8 is distributed uniformly among the channels.

## 2.10 Operation Data

The reactor is at the beginning of cycle 1 (zero EFPD: no Xenon or Iodine, no fuel depletion). The steady state operation data are defined in Table 2.8.

## 2.11 Heat Exchange Correlations

The conductance of the helium-filled gap between fuel and cladding ( $k_{\text{gap}}$ ) is assumed to be constant

$$k_{\text{gap}} = 10^4 \text{ W/m}^2 \text{ } ^\circ\text{K}$$

The heat exchange coefficient between cladding and moderator has to be calculated using own correlations (e.g. Dittus-Boelter and Jens-Lottes), except for case "C", where it is set to a given constant value (see 3.3 below).

## 2.11 Pressure Drops

A homogeneous core pressure of 155 bar is assumed.

### 3. PROBLEM DESCRIPTION

#### 3.1 Nature of the Problem

The transient to be analyzed as a function of time in 3-D or 1-D is generated by the withdrawal of control rods banks from an initially critical core at hot zero power (HZP). The withdrawal speed is a typical bounding value.

The reactor trip signal is generated when the power level reaches a typical high flux level; the rods begin to fall after a conventional delay (a typical conservative value).

#### 3.2 Initial Steady State Calculation

In order to achieve an effective multiplication factor of one, the critical steady state parameters of the reactor core have to be found from a search calculation of the critical boron concentration for the given thermal power and CA configuration.

#### 3.3 Transient calculations

Four cases are submitted for the benchmark calculations. In each case, the transient is to be analyzed until 10 seconds after reactor trip signal. Common part of data is the following (typical for licensing evaluation):

- rod banks are withdrawn from their maximum insertion (i.e. 37.7 cm above the bottom of the lower reflector), at 72 steps / minute;
- initial power level is  $10^{-13}$  times nominal power (0.2775 mW);
- rods begin to fall 0.6 seconds after fission power reached 35 % of nominal, with a constant speed (2.2 seconds for 228 steps); rod banks undergoing withdrawal as well as other banks does participate to scram;
- moderator inlet conditions (flow, pressure, temperature, boron concentration) are constant during the transient.

Specific data for each case:

- case A: bank D withdrawal  
other banks (C,B,A,S) are fully withdrawn until scram
- case B: banks B and C withdrawal  
banks A and D remains fully inserted  
other banks (S) are fully withdrawn until scram
- case C: same as case B, except that the heat transfer coefficient between cladding and water is set constant (30 000 W/m<sup>2</sup>/K)
- case D: banks A and B withdrawal (most peripheral rods)  
banks C and D remains fully inserted  
other banks (S) are fully withdrawn until scram

#### 3.4 Rods configuration

Configuration is defined on figure 2.2; it corresponds to a typical disposition.

## 4. OUTPUT DESCRIPTION

### 4.1 Initial steady state

- B1: critical boron concentration, in ppm
- B2: radially averaged axial power distribution, for 16 axial nodes, normalized to core average power
- B3: axially averaged radial power distribution, for 26 radial nodes (octant core), normalized to core average power
- B4: radial power distribution at axial layer number 6, for 26 radial nodes (octant core), normalized to core average power
- B5: radial power distribution at axial layer number 13, for 26 radial nodes (octant core), normalized to core average power
- B6: envelope axial power distribution  $F_q(z)$ , for 16 axial nodes, calculated as local maximum/average linear fission power density

### 4.2 Transient core averaged results (time histories)

- C1: fission power, relative to average nominal value
- C2: coolant heating, power transmitted to coolant, relative to average nominal value
- C3: coolant outlet temperature, in °C
- C4: fuel Doppler temperature, in °C

### 4.3 Transient hot pellet results (time histories)

These results are calculated using the finest available power distribution. As stated in 2.7, fuel assemblies are considered as homogeneous for the neutronic problem; "finest distribution" should thus not be based on pin and guide tubes modelling.

- D1: fission power, local power density, relative to average nominal value
- D2: coolant heating, linear power density, relative to average nominal value
- D3: coolant temperature at outlet of hot channel, in °C
- D4: heat exchange coefficient between cladding and moderator, in  $W/m^2/°C$
- D5: fuel enthalpy, pellet averaged, in J/Kg
- D6: fuel temperature at pellet centerline,

in °C

- D7: cladding outer surface temperature,  
in °C

#### 4.4 Snapshots at time of power maximum

- E1: fission power,  
relative to average nominal power
- E2: radially averaged axial power distribution,  
for 16 axial nodes, normalized to core average power
- E3: axially averaged radial power distribution,  
for 26 radial nodes (octant core), normalized to core average power
- E4: radial power distribution at axial layer number 6,  
for 26 radial nodes (octant core), normalized to core average power
- E5: radial power distribution at axial layer number 13,  
for 26 radial nodes (octant core), normalized to core average power
- E6: envelope axial power distribution  $F_q(z)$ ,  
for 16 axial nodes, calculated as local maximum/average linear fission power density

## 5. OUTPUT FORMAT

### 5.1 General information

Results may be sent via EMAIL to FRAIKIN@TRACTEBEL.BE or on diskette, to Roger FRAIKIN, TRACTEBEL, Avenue Ariane, 7, B-1200 BRUSSELS (Belgium).

Diskette should be in PC 3.5" (720KB or 1.44MB) or in PC 5.25" (360KB or 1.2KB) format, containing one text (ASCII) file for each case, respectively named: RESULTS.A, RESULTS.B, RESULTS.C and RESULTS.D

Contents should be typed as close as possible to sample format.

#### Remarks:

- time histories consist in couples of [time, value], one per line, starting at 0 s, up to trip signal time + 10 s,
- a plot of time histories would be much appreciated for a first quick comparison of the transient results,
- maximum and envelope have to be calculated using finest available flux reconstruction method (see 4.3 above).
- radial and axial profiles should be given according to Figures 5.1 and 5.2 forms.

### 5.2 Output sample

NEA / NSC PWR CORE TRANSIENT BENCHMARK  
UNCONTROLLED WITHDRAWAL OF CONTROL RODS AT ZERO POWER  
RESULTS FROM CODE "XXXXXXXXX"

A) CASE: A

B) STEADY STATE RESULTS

B1) critical boron concentration: 9999.9 ppm

B2) radially averaged axial power distribution:

```
0.9999 0.9999 0.9999 0.9999 0.9999 0.9999 0.9999 0.9999
0.9999 0.9999 0.9999 0.9999 0.9999 0.9999 0.9999 0.9999
```

B3) axially averaged radial power distribution:

```
                0.9999 0.9999
              0.9999 0.9999 0.9999 0.9999
            0.9999 0.9999 0.9999 0.9999 0.9999
          0.9999 0.9999 0.9999 0.9999 0.9999 0.9999
        0.9999 0.9999 0.9999 0.9999 0.9999 0.9999 0.9999
```

B4) radial power distribution at axial layer number 6:

```
                0.9999 0.9999
              0.9999 0.9999 0.9999 0.9999
            0.9999 0.9999 0.9999 0.9999 0.9999
          0.9999 0.9999 0.9999 0.9999 0.9999 0.9999
        0.9999 0.9999 0.9999 0.9999 0.9999 0.9999 0.9999
```

B5) radial power distribution at axial layer number 13:

```
          0.9999 0.9999
        0.9999 0.9999 0.9999 0.9999
      0.9999 0.9999 0.9999 0.9999 0.9999
    0.9999 0.9999 0.9999 0.9999 0.9999 0.9999 0.9999
  0.9999 0.9999 0.9999 0.9999 0.9999 0.9999 0.9999 0.9999
```

B6) envelope axial power distribution Fq(z):

```
0.9999 0.9999 0.9999 0.9999 0.9999 0.9999 0.9999 0.9999
0.9999 0.9999 0.9999 0.9999 0.9999 0.9999 0.9999 0.9999
```

C) TRANSIENT CORE AVERAGED RESULTS (TIME HISTORIES)

C1) fission power:

```
0.000 9.9999E+99
...
99.999 9.9999E+99
```

C2) coolant heating:

```
0.000 9.9999E+99
...
99.999 9.9999E+99
```

C3) coolant outlet temperature:

```
0.000 9999.99
...
99.999 9999.99
```

C4) fuel Doppler temperature:

```
0.000 9999.99
...
99.999 9999.99
```

D) TRANSIENT HOT PELLETT RESULTS (TIME HISTORIES)

D1) fission power:

```
0.000 9.9999E+99
...
99.999 9.9999E+99
```

D2) coolant heating:

```
0.000 9.9999E+99
...
99.999 9.9999E+99
```

D3) coolant temperature at outlet of hot channel:

```
0.000 9999.99
...
99.999 9999.99
```

D4) heat exchange coefficient between cladding and moderator

```
0.000 9.9999E+99
...
99.999 9.9999E+99
```

D5) fuel enthalpy:

```
0.000 9.9999E+99
...
99.999 9.9999E+99
```

D6) fuel temperature at pellet centerline:  
 0.000 9999.99  
 \*\*\*  
 99.999 9999.99

D7) cladding outer surface temperature:  
 0.000 9999.99  
 \*\*\*  
 99.999 9999.99

E) SNAPSHOTS AT TIME OF POWER MAXIMUM

E1) fission power:  
 9.9999E+99

E2) radially averaged axial power distribution:  
 0.9999 0.9999 0.9999 0.9999 0.9999 0.9999 0.9999 0.9999  
 0.9999 0.9999 0.9999 0.9999 0.9999 0.9999 0.9999 0.9999

E3) axially averaged radial power distribution:  
 0.9999 0.9999  
 0.9999 0.9999 0.9999 0.9999  
 0.9999 0.9999 0.9999 0.9999 0.9999  
 0.9999 0.9999 0.9999 0.9999 0.9999 0.9999 0.9999  
 0.9999 0.9999 0.9999 0.9999 0.9999 0.9999 0.9999 0.9999

E4) radial power distribution at axial layer number 6:  
 0.9999 0.9999  
 0.9999 0.9999 0.9999 0.9999  
 0.9999 0.9999 0.9999 0.9999 0.9999  
 0.9999 0.9999 0.9999 0.9999 0.9999 0.9999 0.9999  
 0.9999 0.9999 0.9999 0.9999 0.9999 0.9999 0.9999 0.9999

E5) radial power distribution at axial layer number 13:  
 0.9999 0.9999  
 0.9999 0.9999 0.9999 0.9999  
 0.9999 0.9999 0.9999 0.9999 0.9999  
 0.9999 0.9999 0.9999 0.9999 0.9999 0.9999 0.9999  
 0.9999 0.9999 0.9999 0.9999 0.9999 0.9999 0.9999 0.9999

E6) envelope axial power distribution:  
 0.9999 0.9999 0.9999 0.9999 0.9999 0.9999 0.9999 0.9999  
 0.9999 0.9999 0.9999 0.9999 0.9999 0.9999 0.9999 0.9999

## 6. TABLES

Table 2.1 Velocities and energy release of prompt neutrons

Table 2.2 Decay constant and fractions of delayed neutrons

Table 2.3 Definition of compositions

Table 2.4 Key to macroscopic cross sections tables

Table 2.5 Cross sections  $\Delta\Sigma_{CA}$  of control assemblies

Table 2.6.xx Cross sections and their derivatives for composition number xx

Table 2.7 Data of the subassembly (FA) geometry

Table 2.8 Steady state operation data

**NEA-NSC PWR CORE TRANSIENT BENCHMARK  
UNCONTROLLED WITHDRAWAL OF CONTROL RODS AT ZERO POWER**

**Table 2.1 Velocities and energy release of prompt neutrons**

	fast energy group	thermal energy group
neutron velocity (cm/s)	0.28 10 <sup>8</sup>	0.44 10 <sup>6</sup>
energy release (Ws/fission)	0.3213 10 <sup>-10</sup>	0.3206 10 <sup>-10</sup>

**Table 2.2 Decay constant and fractions of delayed neutrons**

group	decay constant (s <sup>-1</sup> )	relative fraction of delayed neutrons
1	0.0128	0.034
2	0.0318	0.200
3	0.1190	0.183
4	0.3181	0.404
5	1.4027	0.145
6	3.9286	0.034

total fraction of delayed neutrons: 0.76 %

**Table 2.3 Definition of compositions**

composition.	characteristics
1	axial reflector
2	radial reflector
3	radial reflector re-entrant corner
4	2.1 w/o
5	2.6 w/o
6	3.1 w/o
7	2.6 w/o, 12 burnable absorber rods (BA)
8	2.6 w/o, 16 BA
9	2.6 w/o, 20 BA
10	3.1 w/o, 12 BA
11	3.1 w/o, 16 BA

**NEA-NSC PWR CORE TRANSIENT BENCHMARK  
UNCONTROLLED WITHDRAWAL OF CONTROL RODS AT ZERO POWER**

**Table 2.4 Key to macroscopic cross section tables**

$\Sigma_{tr,1}$	$\Sigma_{1 \rightarrow 2}$	$\Sigma_{a,1}$	$v\Sigma_{f,1}$	$\Sigma_{f,1}$
$\Sigma_{tr,2}$	$\Sigma_{a,2}$	$v\Sigma_{f,2}$	$\Sigma_{f,2}$	Comp.Nr.
$\partial\Sigma_{tr,1}/\partial c$	$\partial\Sigma_{1 \rightarrow 2}/\partial c$	$\partial\Sigma_{a,1}/\partial c$	$\partial v\Sigma_{f,1}/\partial c$	$\partial\Sigma_{f,1}/\partial c$
$\partial\Sigma_{tr,2}/\partial c$	$\partial\Sigma_{a,2}/\partial c$	$\partial v\Sigma_{f,2}/\partial c$	$\partial\Sigma_{f,2}/\partial c$	$c_o$
$\partial\Sigma_{tr,1}/\partial T_M$	$\partial\Sigma_{1 \rightarrow 2}/\partial T_M$	$\partial\Sigma_{a,1}/\partial T_M$	$\partial v\Sigma_{f,1}/\partial T_M$	$\partial\Sigma_{f,1}/\partial T_M$
$\partial\Sigma_{tr,2}/\partial T_M$	$\partial\Sigma_{a,2}/\partial T_M$	$\partial v\Sigma_{f,2}/\partial T_M$	$\partial\Sigma_{f,2}/\partial T_M$	$T_{Mo}$
$\partial\Sigma_{tr,1}/\partial \rho$	$\partial\Sigma_{1 \rightarrow 2}/\partial \rho$	$\partial\Sigma_{a,1}/\partial \rho$	$\partial v\Sigma_{f,1}/\partial \rho$	$\partial\Sigma_{f,1}/\partial \rho$
$\partial\Sigma_{tr,2}/\partial \rho$	$\partial\Sigma_{a,2}/\partial \rho$	$\partial v\Sigma_{f,2}/\partial \rho$	$\partial\Sigma_{f,2}/\partial \rho$	$\rho_o$
$\partial\Sigma_{tr,1}/\partial \sqrt{T_F}$	$\partial\Sigma_{1 \rightarrow 2}/\partial \sqrt{T_F}$	$\partial\Sigma_{a,1}/\partial \sqrt{T_F}$	$\partial v\Sigma_{f,1}/\partial \sqrt{T_F}$	$\partial\Sigma_{f,1}/\partial \sqrt{T_F}$
$\partial\Sigma_{tr,2}/\partial \sqrt{T_F}$	$\partial\Sigma_{a,2}/\partial \sqrt{T_F}$	$\partial v\Sigma_{f,2}/\partial \sqrt{T_F}$	$\partial\Sigma_{f,2}/\partial \sqrt{T_F}$	$T_{Fo}$

where

Comp.Nr	is the composition number	[1-11]
c	is the boron concentration	[ppm]
$\rho$	is the water density	[g/cm <sup>3</sup> ],
TM	is the moderator temperature	[°C],
TF	is the fuel temperature ("Doppler Temperature")	[K]

Reference values are labelled with subscript "o".

macroscopic cross sections are in units of cm<sup>-1</sup>

the meanings of the indices of cross sections are:

1,2	fast or thermal neutron group
tr	transport
1→2	scattering from group 1 into group 2
a	absorption
f	fission
v	number of neutrons per fission

The transport cross section is related to the diffusion constant D by

$$D = 1 / (3 \Sigma_{tr})$$

**NEA-NSC PWR CORE TRANSIENT BENCHMARK  
UNCONTROLLED WITHDRAWAL OF CONTROL RODS AT ZERO POWER**

**Table 2.5 CA cross section increments**

.373220E-02	-.319253E-02	.247770E-02	-.102786E-03	-.377989E-04	
-.219926E-01	.255875E-01	-.282319E-02	-.115483E-02	absorber type1	(B,C,D,S)
.374092E-02	-.314239E-02	.242926E-02	-.122634E-03	-.459250E-04	
-.167503E-01	.256478E-01	-.328086E-02	-.134262E-02	absorber type2	(A)
.697102E-02	-.119034E-02	.879034E-04		driver device	
-.113498E-01	.170043E-02				

( $\Sigma_{f1,2}$  and  $\nu\Sigma_{f1,2}$  are defined as zero in reflector region)

**Table 2.6.1 Cross sections and their derivatives for composition number 1**

.532058E-01	.264554E-01	.373279E-03	.000000E+00	.000000E+00
.386406E+00	.177215E-01	.000000E+00	.000000E+00	1
.611833E-07	.791457E-09	.187731E-06	.000000E+00	.000000E+00
.517535E-05	.102635E-04	.000000E+00	.000000E+00	1200.2
.000000E+00	.000000E+00	.000000E+00	.000000E+00	.000000E+00
.000000E+00	.000000E+00	.000000E+00	.000000E+00	306.6
.745756E-01	.371310E-01	.207688E-03	.000000E+00	.000000E+00
.533634E+00	.758421E-02	.000000E+00	.000000E+00	0.7125
.000000E+00	.000000E+00	.000000E+00	.000000E+00	.000000E+00
.000000E+00	.000000E+00	.000000E+00	.000000E+00	891.45

**Table 2.6.2 Cross sections and their derivatives for composition number 2**

.295609E+00	.231613E-01	.118782E-02	.000000E+00	.000000E+00
.245931E+01	.252618E+00	.000000E+00	.000000E+00	2
.000000E+00	.000000E+00	.000000E+00	.000000E+00	.000000E+00
.776184E-03	.844695E-04	.000000E+00	.000000E+00	1200.2
.000000E+00	.000000E+00	.000000E+00	.000000E+00	.000000E+00
.000000E+00	.000000E+00	.000000E+00	.000000E+00	306.6
.000000E+00	.000000E+00	.000000E+00	.000000E+00	.000000E+00
.000000E+00	.000000E+00	.000000E+00	.000000E+00	0.7125
.000000E+00	.000000E+00	.000000E+00	.000000E+00	.000000E+00
.000000E+00	.000000E+00	.000000E+00	.000000E+00	891.45

**Table 2.6.3 Cross sections and their derivatives for composition number 3**

.295609E+00	.200808E-01	.118782E-02	.000000E+00	.000000E+00
.245931E+01	.252618E+00	.000000E+00	.000000E+00	3
.000000E+00	.000000E+00	.000000E+00	.000000E+00	.000000E+00
.776184E-03	.844695E-04	.000000E+00	.000000E+00	1200.2
.000000E+00	.000000E+00	.000000E+00	.000000E+00	.000000E+00
.000000E+00	.000000E+00	.000000E+00	.000000E+00	306.6
.000000E+00	.000000E+00	.000000E+00	.000000E+00	.000000E+00
.000000E+00	.000000E+00	.000000E+00	.000000E+00	0.7125
.000000E+00	.000000E+00	.000000E+00	.000000E+00	.000000E+00
.000000E+00	.000000E+00	.000000E+00	.000000E+00	891.45

**NEA-NSC PWR CORE TRANSIENT BENCHMARK  
UNCONTROLLED WITHDRAWAL OF CONTROL RODS AT ZERO POWER**

**Table 2.6.4 Cross sections and their derivatives for composition number 4**

.222117E+00	.182498E-01	.871774E-02	.498277E-02	.190224E-02
.803140E+00	.652550E-01	.839026E-01	.343581E-01	4
.347809E-07	-.108590E-06	.128505E-06	-.112099E-08	-.548361E-09
-.976510E-05	.708807E-05	-.243045E-05	-.995273E-06	1200.2
-.203310E-05	.809676E-06	.212191E-06	.124709E-06	.445177E-07
-.108674E-03	-.315597E-04	-.416439E-04	-.170531E-04	306.6
.135665E+00	.293195E-01	.155185E-02	.920694E-03	.318680E-03
.992628E+00	.252662E-01	.247746E-01	.101452E-01	0.7125
-.309197E-04	-.275536E-04	-.349709E-04	.640134E-06	.222662E-06
-.137292E-03	-.371806E-04	-.563037E-04	-.230564E-04	891.45

**Table 2.6.5 Cross sections and their derivatives for composition number 5**

.221914E+00	.180040E-01	.906133E-02	.557659E-02	.214498E-02
.795538E+00	.723354E-01	.998629E-01	.408938E-01	5
.353826E-07	-.106951E-06	.126709E-06	-.167880E-08	-.777980E-09
-.850169E-05	.682311E-05	-.272445E-05	-.111566E-05	1200.2
-.198080E-05	.858474E-06	.226000E-06	.135145E-06	.488317E-07
-.906150E-04	-.321435E-04	-.453102E-04	-.185545E-04	306.6
.135748E+00	.292696E-01	.161491E-02	.964160E-03	.336573E-03
.981985E+00	.286667E-01	.314993E-01	.128990E-01	0.7125
-.308607E-04	-.276766E-04	.351798E-04	.997431E-06	.369389E-06
-.117481E-03	-.377039E-04	-.604155E-04	-.247402E-04	891.45

**Table 2.6.6 Cross sections and their derivatives for composition number 6**

.221715E+00	.177670E-01	.938496E-02	.615047E-02	.237972E-02
.789253E+00	.789203E-01	.114667E+00	.469561E-01	6
.359838E-07	-.105374E-06	.124986E-06	-.221038E-08	-.996653E-09
-.746251E-05	.659798E-05	-.295883E-05	-.121164E-05	1200.2
-.192434E-05	.903494E-06	.239939E-06	.149084E-06	.545978E-07
-.762786E-04	-.323776E-04	-.478475E-04	-.195937E-04	306.6
.135827E+00	.292154E-01	.168015E-02	.101410E-02	.357207E-03
.972267E+00	.319571E-01	.381097E-01	.156060E-01	0.7125
-.309165E-04	-.278390E-04	.353841E-04	.141847E-05	.542384E-06
-.101337E-03	-.377558E-04	-.630960E-04	-.258379E-04	891.45

**Table 2.6.7 Cross sections and their derivatives for composition number 7**

.222039E+00	.171381E-01	.931692E-02	.555010E-02	.213629E-02
.776230E+00	.796328E-01	.985576E-01	.403596E-01	7
.337806E-07	-.100873E-06	.119869E-06	-.171323E-08	-.777980E-09
-.673744E-05	.629310E-05	-.255359E-05	-.104561E-05	1200.2
-.269634E-05	.701311E-06	.248530E-06	.140773E-06	.488317E-07
-.762435E-04	-.300119E-04	-.420202E-04	-.172074E-04	306.6
.131033E+00	.282489E-01	.168397E-02	.981951E-03	.336573E-03
.934697E+00	.314240E-01	.351588E-01	.144016E-01	0.7125
-.313746E-04	-.273550E-04	.348699E-04	.945431E-06	.369389E-06
-.108271E-03	-.372748E-04	-.579662E-04	-.237320E-04	891.45

**NEA-NSC PWR CORE TRANSIENT BENCHMARK  
UNCONTROLLED WITHDRAWAL OF CONTROL RODS AT ZERO POWER**

**Table 2.6.8 Cross sections and their derivatives for composition number 8**

.222083E+00	.168501E-01	.940032E-02	.554083E-02	.213318E-02
.769969E+00	.821087E-01	.980059E-01	.401338E-01	8
.332495E-07	-.988578E-07	.117585E-06	-.172421E-08	-.793325E-09
-.619725E-05	.611904E-05	-.248880E-05	-.101904E-05	1200.2
-.307905E-05	.617380E-06	.261854E-06	.143235E-06	.522555E-07
-.733397E-04	-.291929E-04	-.407701E-04	-.166956E-04	306.6
.129379E+00	.278895E-01	.171972E-02	.988437E-03	.346474E-03
.918171E+00	.324715E-01	.363251E-01	.148808E-01	0.7125
-.315503E-04	-.272381E-04	.347274E-04	.926078E-06	.339044E-06
-.105521E-03	-.371808E-04	-.571108E-04	-.233804E-04	891.45

**Table 2.6.9 Cross sections and their derivatives for composition number 9**

.222127E+00	.165626E-01	.948286E-02	.553137E-02	.213003E-02
.763813E+00	.845912E-01	.974109E-01	.398902E-01	9
.327201E-07	-.968489E-07	.115319E-06	-.173502E-08	-.796917E-09
-.568220E-05	.594711E-05	-.242240E-05	-.991817E-06	1200.2
-.353877E-05	.516547E-06	.274313E-06	.146019E-06	.534283E-07
-.713711E-04	-.283041E-04	-.394319E-04	-.161475E-04	306.6
.127682E+00	.275202E-01	.174989E-02	.995175E-03	.349236E-03
.901293E+00	.335945E-01	.374499E-01	.153431E-01	0.7125
-.317281E-04	-.271169E-04	.346026E-04	.905802E-06	.330425E-06
-.102525E-03	-.370201E-04	-.561543E-04	-.229872E-04	891.45

**Table 2.6.10 Cross sections and their derivatives for composition number 10**

.221836E+00	.169043E-01	.963720E-02	.612382E-02	.237097E-02
.770705E+00	.861187E-01	.113241E+00	.463724E-01	10
.343859E-07	-.993312E-07	.118186E-06	-.224335E-08	-.996653E-09
-.586898E-05	.608443E-05	-.277657E-05	-.113696E-05	1200.2
-.263907E-05	.744320E-06	.264289E-06	.155858E-06	.545978E-07
-.639554E-04	-.303509E-04	-.444431E-04	-.181997E-04	306.6
.131116E+00	.281877E-01	.175528E-02	.103522E-02	.357207E-03
.924925E+00	.349853E-01	.420693E-01	.172298E-01	0.7125
-.314192E-04	-.275049E-04	.350637E-04	.135642E-05	.542384E-06
-.938886E-04	-.371403E-04	-.605052E-04	-.247739E-04	891.45

**Table 2.6.11 Cross sections and their derivatives for composition number 11**

.221878E+00	.166175E-01	.971937E-02	.611444E-02	.236781E-02
.764704E+00	.885488E-01	.112635E+00	.461246E-01	11
.338559E-07	-.973291E-07	.115917E-06	-.225369E-08	-.101112E-08
-.538345E-05	.591697E-05	-.270780E-05	-.110878E-05	1200.2
-.302147E-05	.659521E-06	.279060E-06	.158814E-06	.586765E-07
-.616984E-04	-.295626E-04	-.431588E-04	-.176738E-04	306.6
.129463E+00	.278259E-01	.179499E-02	.104291E-02	.368921E-03
.908456E+00	.361032E-01	.433215E-01	.177435E-01	0.7125
-.315908E-04	-.273835E-04	.349119E-04	.133336E-05	.506596E-06
-.917126E-04	-.369909E-04	-.596284E-04	-.244141E-04	891.45

**NEA-NSC PWR CORE TRANSIENT BENCHMARK  
UNCONTROLLED WITHDRAWAL OF CONTROL RODS AT ZERO POWER**

**Table 2.7. Data of the subassembly (FA) geometry**

Pellet diameter:	8.239	mm
Clad diameter (outside):	9.517	mm
Clad wall thickness:	0.571	mm
FR pitch:	12.655	mm
Guide tube diameter (outside):	12.259	mm
Guide tube diameter (inside):	11.448	mm
Geometry:	17 x 17	
Number of fuel pins:	264	
Number of guide tubes:	25	

**Table 2.8. Steady state operation data**

Core thermal output:	2775	MW
Core inlet temperature:	286	°C
Core pressure:	155	bar
Net mass flow through core:	12893	kg/s

## 7. FIGURES

Figure 2.1 Cross section of the reactor core

Figure 2.2 Arrangement of control rods

Figure 2.3 Composition numbers in axial layers 1 and 18 (bottom and top reflector)

Figure 2.4 Composition numbers in axial layer 2 (bottom layer of active core)

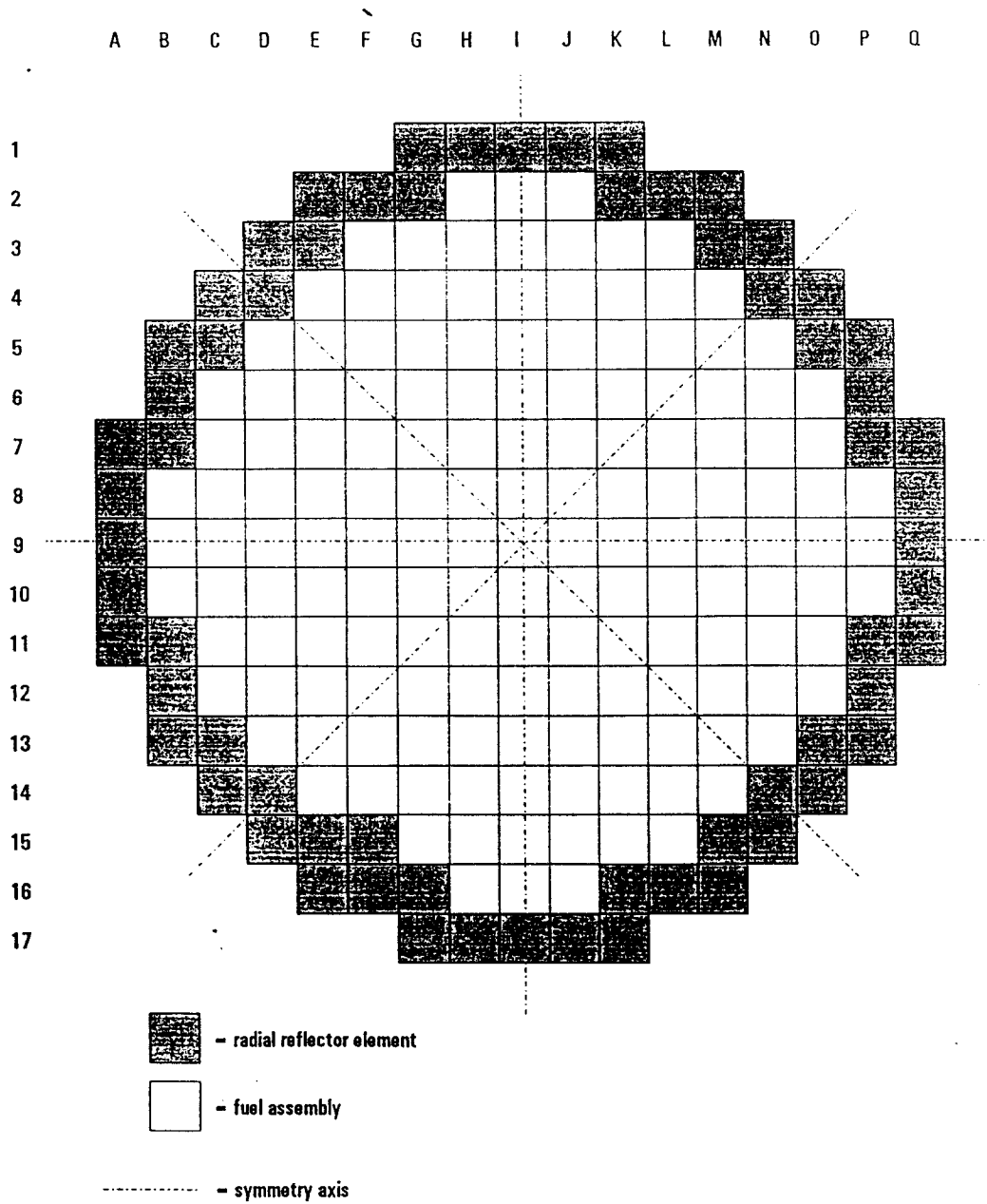
Figure 2.5 Composition numbers in axial layer 3 through 17 (active core)

Figure 5.1 Form for power axial distribution

Figure 5.2 Form for power radial distribution

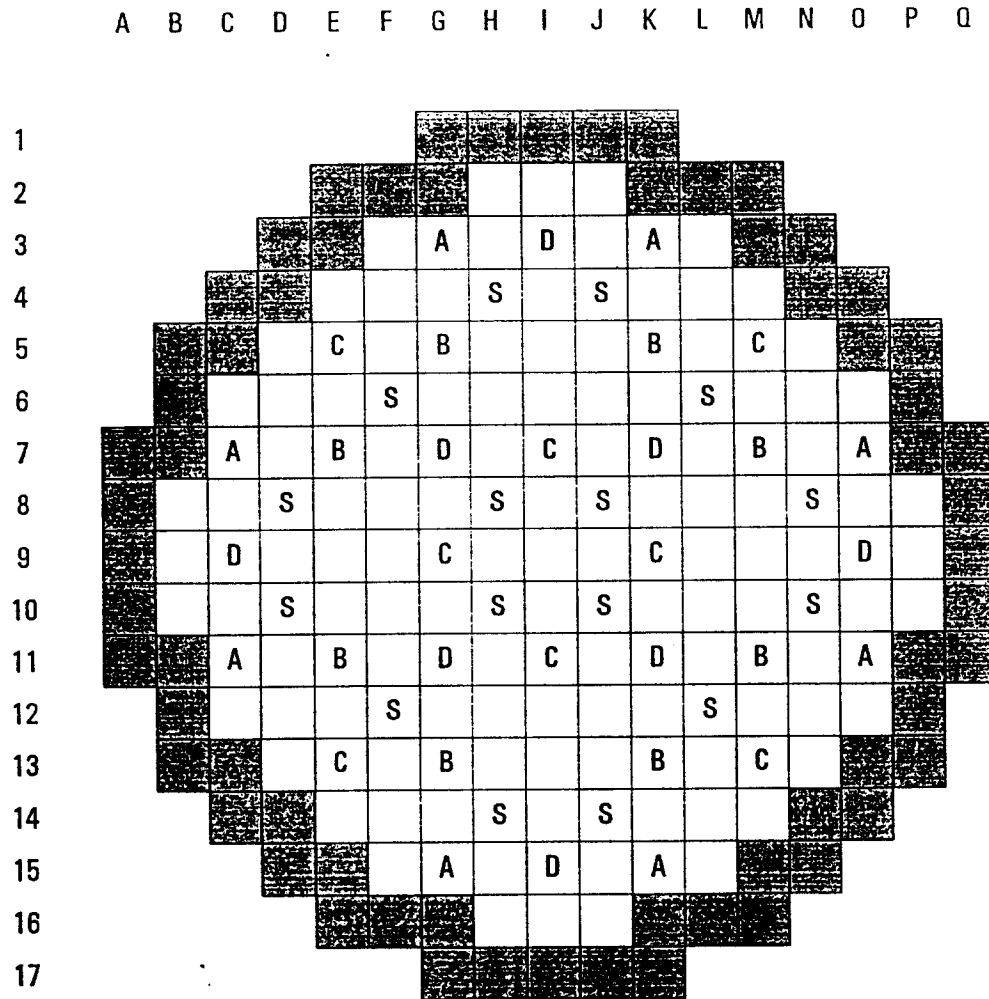
NEA-NSC PWR CORE TRANSIENT BENCHMARK  
UNCONTROLLED WITHDRAWAL OF CONTROL RODS AT ZERO POWER

Figure 2.1 Cross section of the reactor core



NEA-NSC PWR CORE TRANSIENT BENCHMARK  
 UNCONTROLLED WITHDRAWAL OF CONTROL RODS AT ZERO POWER

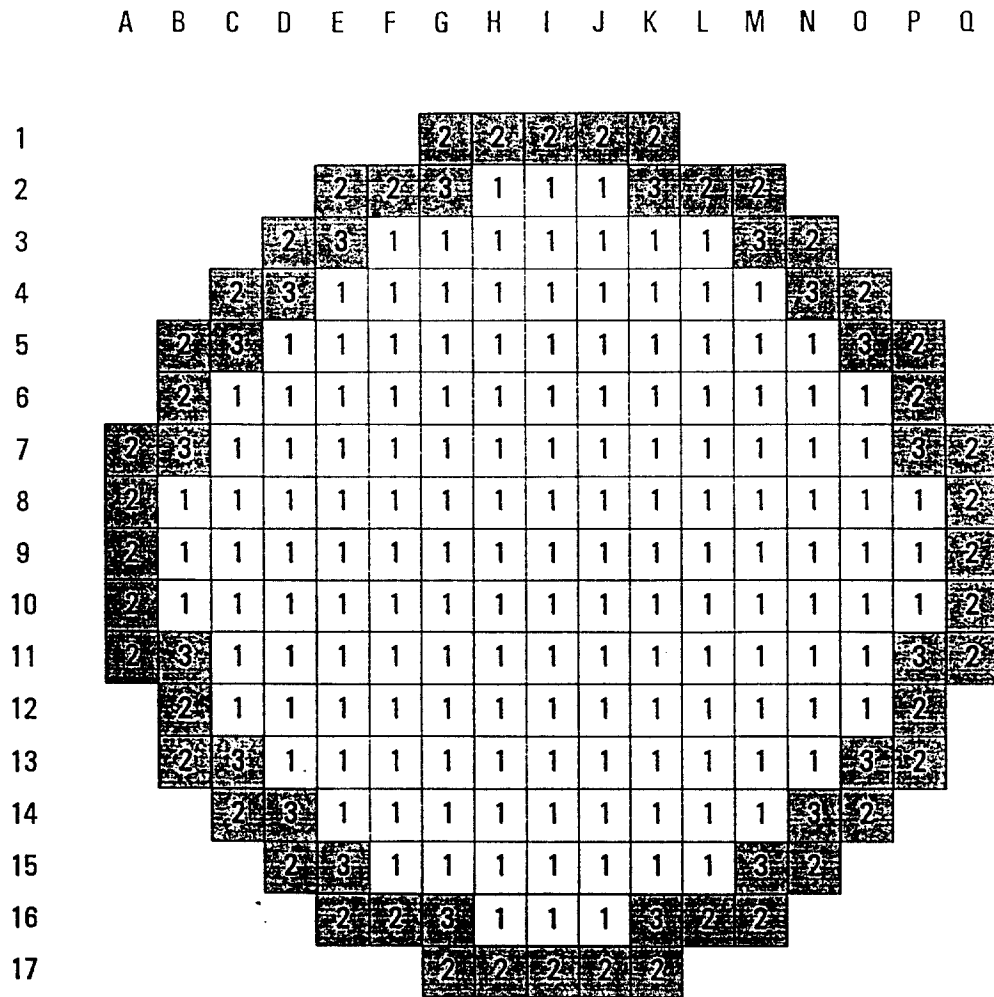
Figure 2.2 Arrangement of control rods



B, C, D, S: "Type 1" absorbers, i.e. located in 2.1 % enriched FAs (Comp 4)  
 A: "Type 2" absorbers, i.e. located in 3.1 % enriched FAs (Comp 6)

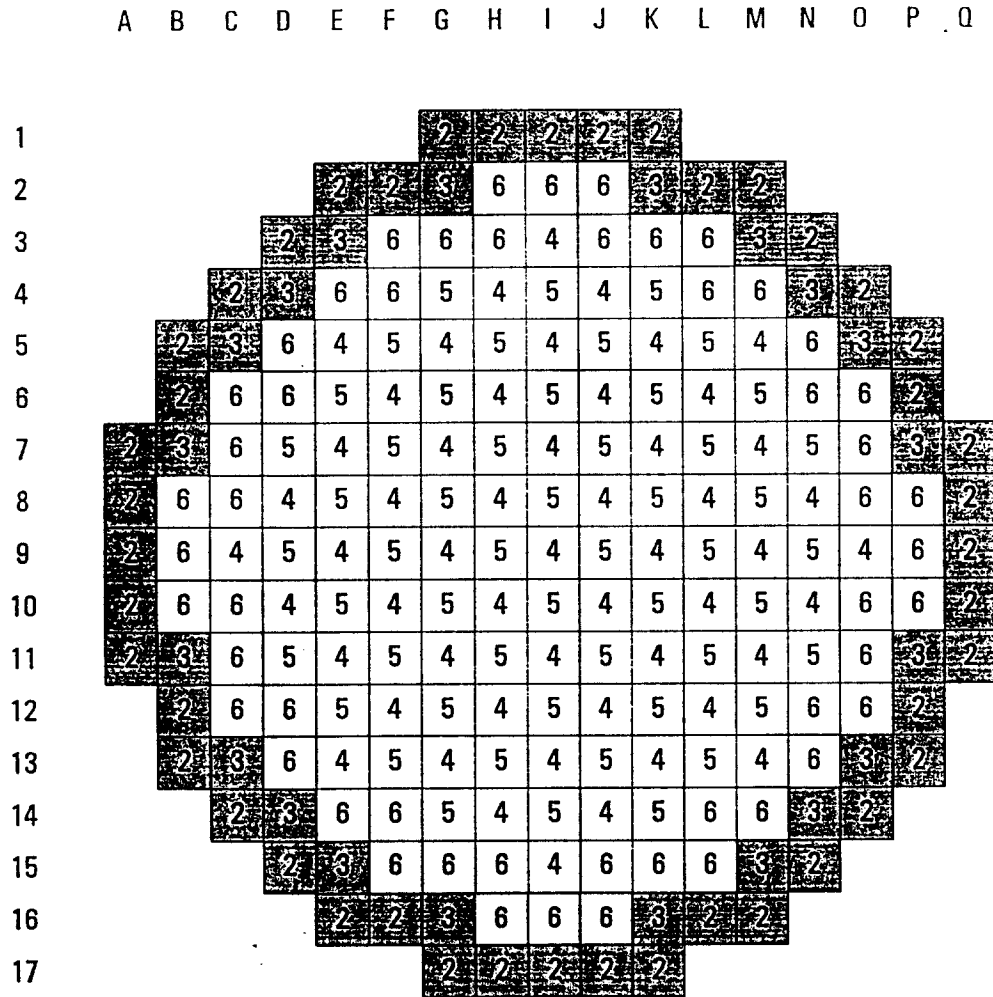
NEA-NSC PWR CORE TRANSIENT BENCHMARK  
UNCONTROLLED WITHDRAWAL OF CONTROL RODS AT ZERO POWER

**Figure 2.3** Composition numbers in axial layers 1 and 18 (bottom and top reflector)



NEA-NSC PWR CORE TRANSIENT BENCHMARK  
UNCONTROLLED WITHDRAWAL OF CONTROL RODS AT ZERO POWER

Figure 2.4 Composition numbers in axial layer 2 (bottom layer of active core)



NEA-NSC PWR CORE TRANSIENT BENCHMARK  
UNCONTROLLED WITHDRAWAL OF CONTROL RODS AT ZERO POWER

Figure 2.5 Composition numbers in axial layer 3 through 17 (active core)

	A	B	C	D	E	F	G	H	I	J	K	L	M	N	O	P	Q						
1							2	2	2	2	2												
2							2	2	3	6	6	6	3	2	2								
3							2	3	6	6	11	4	11	6	6	3	2						
4							2	3	6	10	8	4	7	4	8	10	6	3	2				
5							2	3	6	4	8	4	8	4	8	4	8	4	6	3	2		
6							2	6	10	8	4	8	4	9	4	8	4	8	10	6	2		
7							2	3	6	8	4	8	4	8	4	8	4	8	4	8	6	3	2
8							2	6	11	4	8	4	8	4	9	4	8	4	8	4	11	6	2
9							2	6	4	7	4	9	4	9	4	9	4	9	4	7	4	6	2
10							2	6	11	4	8	4	8	4	9	4	8	4	8	4	11	6	2
11							2	3	6	8	4	8	4	8	4	8	4	8	4	8	6	3	2
12							2	6	10	8	4	8	4	9	4	8	4	8	4	10	6	2	
13							2	3	6	4	8	4	8	4	8	4	8	4	6	3	2		
14							2	3	6	10	8	4	7	4	8	10	6	3	2				
15							2	3	6	6	11	4	11	6	6	3	2						
16							2	2	3	6	6	6	3	2	2								
17							2	2	2	2	2												

NEA-NSC PWR CORE TRANSIENT BENCHMARK  
UNCONTROLLED WITHDRAWAL OF CONTROL RODS AT ZERO POWER

**Figure 5.1 Form for power axial distribution**

Layers of the active core

bottom

1	2	3	4	5	6	7	8
9	10	11	12	13	14	15	16

top

**Figure 5.2 Form for power radial distribution**

	I	J	K	L	M	N	O	P
5								
6								
7								
8								
9								

